




Generative Adversarial Network Synthesis for Improved Deep Learning Model Training of Alpine Plants with Fuzzy Structures

Christoph Praschl¹ ^a, Roland Kaiser³ ^b and Gerald Adam Zwettler^{1,2} ^c

¹Research Group Advanced Information Systems and Technology, Research and Development Department, University of Applied Sciences Upper Austria, Softwarepark 11, Hagenberg, 4232, Austria

²Department of Software Engineering, School of Informatics, Communications and Media,

University of Applied Sciences Upper Austria, Softwarepark 11, Hagenberg, 4232, Austria

³ENNACON Environment Nature Consulting KG, Altheim 13, Feldkirchen bei Mattighofen, Austria

Keywords: Plant Cover Image Data Synthesis, Generative Adversarial Networks, Deep Learning Instance Segmentation, Small Training Data Sets.

Abstract: Deep learning approaches are highly influenced by two factors, namely the complexity of the task and the size of the training data set. In terms of both, the extraction of features of low-stature alpine plants represents a challenging domain due to their fuzzy appearance, a great structural variety in plant organs and the high effort associated with acquiring high-quality training data for such plants. For this reason, this study proposes an approach for training deep learning models in the context of alpine vegetation based on a combination of real-world and artificial data synthesised using Generative Adversarial Networks. The evaluation of this approach indicates that synthetic data can be used to increase the size of training data sets. With this at hand, the results and robustness of deep learning models are demonstrated with a U-Net segmentation model. The evaluation is carried out using a cross-validation for three alpine plants, namely *Soldanella pusilla*, *Gnaphalium supinum*, and *Euphrasia minima*. Improved segmentation accuracy was achieved for the latter two species. Dice Scores of 24.16% vs 26.18% were quantified for *Gnaphalium* with 100 real-world training images. In the case of *Euphrasia*, Dice Scores improved from 33.56% to 42.96% using only 20 real-world training images.


1 INTRODUCTION


Over the last decades, the effects of global warming have increased dramatically, resulting in a significantly higher global mean surface temperature than in the pre-industrial period. This process comes with an increased frequency, intensity and duration of climate events. Altogether, the climate crisis leads to a shift of regional climate zones and threatens the fauna and flora on our planet (Shukla et al., 2019). Next to various other regions, this influence has been observed in detail for the European Alps based on, e.g. the retreat of the glaciers (Sommer et al., 2020; Steinbauer et al., 2022) or the upward shift of the potential timber line's mean altitude (Rubel et al., 2017; Körner, 2012). These factors are already causing a pending local decline and retreat of alpine animals (Brunetti et al., 2019; Gobbi et al., 2021) and plant species


(Rumpf et al., 2019; Engler et al., 2011; Dirnböck et al., 2003).

In light of the processes mentioned above, it is essential to conduct objective and quantitative monitoring of the alpine biota over a long period of time in order to accurately track the advance of climate change and its impact on alpine plant diversity (Körner et al., 2022; Körner and Hiltbrunner, 2021). Automating a process such as visual-based long-term monitoring is now possible, thanks to recent improvements in computer vision. In particular, paradigms from deep learning are critical factors in developing such a system. However, these methods have the disadvantage of requiring large amounts of labelled training data to build suitable predictive models (Sun et al., 2017). Since the availability of appropriate training data for the study system is still limited and manual labelling of this input information requires much effort, the data is a sticking point for the practicality of such a system.

The collection of images in alpine environments is resource-intensive due to the need to transport image

^a  <https://orcid.org/0000-0002-9711-4818>

^b  <https://orcid.org/0000-0002-2487-9289>

^c  <https://orcid.org/0000-0002-4966-6853>

acquisition equipment to remote locations. In order to conserve time resources, it is impossible to capture images of alpine plants in huge numbers. Furthermore, to allow objective and unbiased long-term studies, changing light conditions and external weather influences must be avoided during image accession (Eberl and Kaiser, 2020). Artificial data can help to increase the amount of data available to deep learning models. We, therefore, reviewed the use of generative adversarial networks (GAN) (Creswell et al., 2018) for improving U-Net models (Ronneberger et al., 2015) for segmenting fuzzy structures, such as alpine plants, in the context of quantitative monitoring of alpine vegetation over a long period.

2 RELATED WORK

Antoniou et al. proposed to employ generative adversarial networks for the creation of artificial data in addition to classic augmentation strategies such as image transformations or colour adaptations. Like this, they were able to use the so-created data to extend real-world data sets for training additional models; they apply their approach in the context of classification problems (Antoniou et al., 2017). Next to that, Sandfort et al. transferred the idea of utilizing generative adversarial networks to create artificial labelled data to the medical domain. They used this methodology for creating a data set consisting of real-world and augmented data, allowing for improvement in the accuracy of a U-Net segmentation model in the context of computer tomography (CT) scans (Sandfort et al., 2019). Also, Dong et al. go a similar way by creating a combined model architecture called U-Net-GAN, which uses a set of U-Net models as generators of the underlying GAN network in combination with multiple fully convolutional networks as discriminators. This U-Net-GAN architecture is used for the automatic multi-organ segmentation in thorax images in different medical areas such as CT scans, pathology or X-ray images (Dong et al., 2019). A method for training deep learning models in medical domains with small reference data sets is also presented by Zwettler et al. Like in the present work, a U-Net model is iteratively trained for the segmentation of the targeted domain using artificial images created using a GAN network (Zwettler et al., 2020). Similar to the previously mentioned publications, also Schonfeld et al., Guo et al. and Chen et al. combine U-Net segmentation approaches with the generation of training data using GAN networks to increase the number of training images (Schonfeld et al., 2020; Guo et al., 2020; Chen et al., 2021). The

mentioned publications mainly focus on the combination of U-Net models together with GAN architectures in the context of medical applications. They are, for this reason, substantially distinct from the present work. CT and magnetic resonance images differ significantly from RGB images in appearance. On top of that, the structural impression of human organs contrasts with that of plants and is therefore barely comparable. With higher variability in appearance, thinner structures and partly overlapping plant canopies, the vegetation images represent a more challenging domain for precise instance segmentation compared to high-contrast 3D tomography in medicine.

3 MATERIAL

Within an interdisciplinary monitoring and research program for long-term observation of alpine ecosystems in the Hohe Tauern National Park (Austria), a digital true colour image archive in the form of strictly standardised (geo-static, colourfast), high-resolution nadir photos (view vertical to the ground) is being built up. This image data archive provides 215 example RGB images with a size of 600×600 px (10×10 cm in real-world) that are cut-outs of the raw image data (original size: 3000×3000 px equalling 50×50 cm) showing one or multiple alpine plants in an exactly defined area. In order to achieve a consistent and comparable light source, two diffused flashes are used, as well as a shading curtain. Colour charts and grey cards are added to the photographs for calibration. The images are captured with a full-frame camera and a 50 mm lens (Eberl and Kaiser, 2020).

The images of the data set are manually labelled using image classification masks regarding the following plant species: *Euphrasia minima*, *Gnaphalium supinum*, *Leucanthemopsis alpina*, *Potentilla aurea*, *Primula glutinosa*, *Primula minima*, *Salix herbacea*, *Scorzoneroidea helvetica*, *Soldanella pusilla* and *Vaccinium gaultheroides*. Images show partially overlapping occurrences of these species. Figure 1a shows an example image of the training data set, and Figure 1b presents the associated classification mask. The distribution of the different plant species is shown in Table 1.

4 METHODOLOGY

In this work, multiple deep learning models are trained using a U-Net and a progressive growing GAN (PGGAN) model architecture, as proposed by Karras et al. (Karras et al., 2018). By generating an addi-

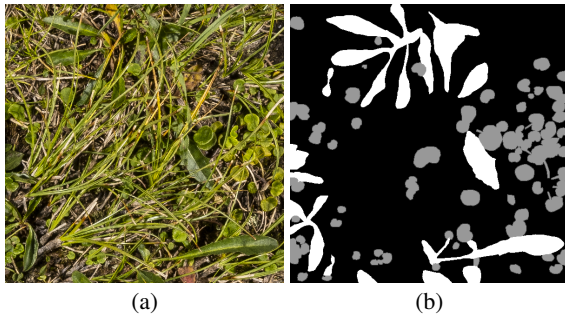


Figure 1: (a) Sample image of the training data set with (b) the associated image mask showing multiple annotated plants species, namely *Scorzonerooides helvetica* in white and *Soldanella pusilla* in grey.

Table 1: Distribution of the alpine plant species in the training data set of 215 images with 77,400,000 pixels in total. Unclassified pixels are interpreted as background pixels.

Plant species	# Images	Relative pixel proportion
<i>Euphrasia minima</i>	23	0.236%
<i>Gnaphalium supinum</i>	103	1.152%
<i>Leucanthemopsis alpina</i>	24	0.416%
<i>Potentilla aurea</i>	6	0.475%
<i>Primula glutinosa</i>	4	0.061%
<i>Primula minima</i>	7	0.276%
<i>Salix herbacea</i>	103	1.954%
<i>Scorzonerooides helvetica</i>	73	6.127%
<i>Soldanella pusilla</i>	162	1.505%
<i>Vaccinium gaultheroides</i>	4	0.616%

tional artificial training set for the U-Net network, the GAN network can increase the diversity of the training set and, thus, improve the segmentation model.

4.1 Data Augmentation

In order to counteract overfitting of the proposed models, a data augmentation strategy is applied to increase the size of the training data set. This enhancement is achieved by applying geometric and intensity transformations to the input images with uniformly distributed random parameters to create variations of the input images and their associated ground truth image masks as follows.

- **Affine Transformation:** Randomly applies affine transformations in the form of rotations and translations to the input image and mask. The images are rotated up to $\pm 90^\circ$ and translated between 0 and $\pm 20\%$ of the image's width along the x-axis and with a height ratio of 0 to $\pm 20\%$ along the y-axis. For the value interpolation, the Lanczos algorithm (Fadnavis, 2014) is used for the RGB input images and the nearest neighbour interpolation (Rukundo and Cao, 2012) is used for the

ground truth masks to avoid noise in the masks' border areas.

- **Gamma Correction:** Applies a gamma correction by manipulating the value channel of the input image in HSV space. The manipulation is done using a factor f between 0.7 and 1.3. This factor results in darker colours with a value below 1 and in brighter colours above 1. It is applied on the value channel like $v' = v^{\frac{1}{f}}$.
- **Convolution:** Either sharpens or blurs the image by applying different convolution filters like Gaussian Blur with a randomly selected kernel size $k \in [3; 7]$ or a sharpening filter with weight w between 1 and 1.2 that is applied like $I_s(x, y) = w * k * I_i(x, y)$ using the kernel $k = \begin{bmatrix} 0 & -1 & 0 \\ -1 & 5 & -1 \\ 0 & -1 & 0 \end{bmatrix}$.
- **Noise:** Adds a normally distributed noise to the image based on a randomly selected standard deviation between 0 and 20 with $I_n(x, y) = I_i(x, y) + \mathcal{N}(x, y)$, $\mathcal{N} \sim (\mu, \sigma^2)$.

Finally, the images and their masks are normalized to a valid space of the unsigned char datatype and are cropped to 3×3 tiles with a size of 128×128 px each, cf. Figure 2b. Only tiles from the centre of the augmentation results are used to avoid black areas from affine transformations such as rotation or translation. To ensure that weak areas (containing background regions as a result of the transformations) are not used for the training, the tiles are also checked according to the background (black) to foreground ratio. The resulting data set is filtered to remove images with a background ratio greater than 0.01%.

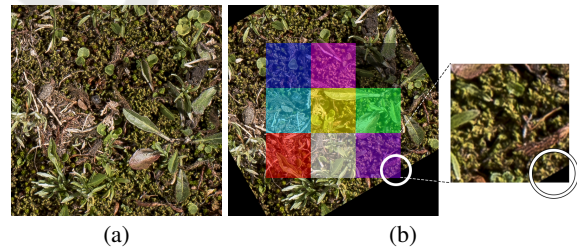


Figure 2: (a) Sample image of the training data set with (b) one associated augmentation result using an affine transformation and noise. Due to the transformation, the bottom right tile contains 3.24% of the background area (marked with a circle) and, for this reason, is not used for the model training. In addition, the finally cropped central tiles are highlighted in colour.

4.2 U-Net Based Multi-Class Image Segmentation

In order to segment alpine plants, multiple U-Net models are trained. Due to the heterogeneous nature of the addressed plants, especially their small stature, the proposed models are intended for segmenting exactly one target plant species like *Euphrasia minima*. This also comes hand in hand with the significant imbalance of the created training data set.

The U-Net architecture consists of five encoders and five decoder steps and thereby expects an unsigned char image with a size of 128×128 px and three channels. Within the contraction path, the images are resized to 64×64 px in the first step and down to 4×4 px in the last step – respectively vice versa in the expansion path.

Within the training phase, an *Adam Optimizer* (Kingma and Ba, 2014) at a learning rate of 0.0001 using a sparse categorical cross entropy loss function and a *batchSize* = 64 are used for up to 100 epochs.

The results of the U-Net model are post-processed by filtering small contours with an area smaller than 0.05% of the image size and using the Grab Cut algorithm (Rother et al., 2004) in an automated way. Based on the initial segmentation mask provided by the U-Net model, a gaussian mixture model is created using the already segmented foreground pixels as “sure” foreground for the post-processing step.

In addition, this segmented mask is extended in a second iteration by morphological transformations to define a “possible” foreground and background. Both dilation steps are applied using a 5×5 kernel. The U-Net post-processing step is shown in Figure 3.

4.3 Progressive Growing Generative Adversarial Network

In this paper, a progressively growing generative adversarial network (PGGAN) is proposed for the expansion of the U-Net training data set. For this purpose, a GAN network is trained with six levels of resolution, starting with 4×4 px and ending with images of 128×128 px. The underlying generator neural network creates images based on a random input using multiple convolutional layers. With the contesting discriminator network, the GAN can iteratively improve its results by determining if the created images are fakes or reals. This architecture is shown based on sample images of multiple stages in Figure 4. The augmented training data set for the network training is resampled to six resolution levels using the Lanczos interpolation algorithm for the RGB data. This step is followed by the nearest neighbour interpolation of

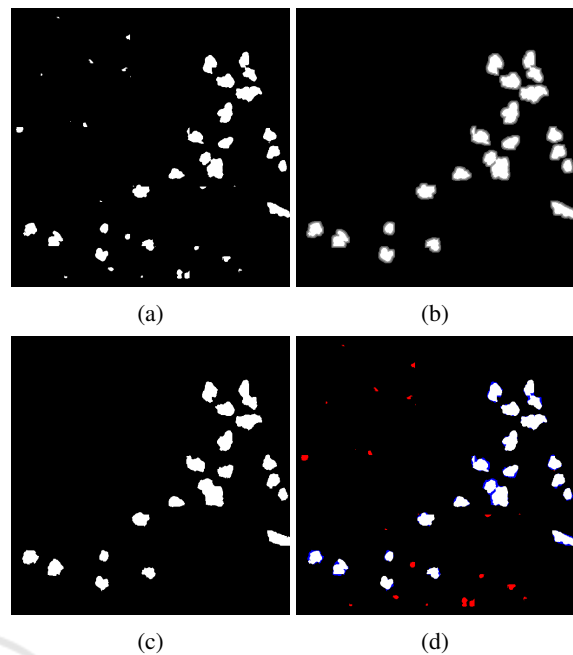


Figure 3: (a) Resulting mask created by the U-Net segmentation, (b) the filtered and dilated version used for the creation of the gaussian mixture model, (c) the application of the Grab Cut algorithm and (d) the comparison of the initial U-Net result and the corresponding post-processed version showing filtered areas in red and extended areas in blue.

the binary masks. The values of the binary masks are equally distributed between the image range of 0 to 255. Within the training, an Adam optimizer with a learning rate of 0.001 is used on four-channel images containing the RGB information and the binary ground truth class mask.

Due to the multi-class nature with partially overlapping plant individuals, the generated result masks of the GAN network are noisy and do not contain unified class regions. Consequently, post-processing is required. To this end, a region-based approach is adopted to extract individual classes from the image by finding the closest class for every pixel. The so-created regions get manipulated using morphological operations with a kernel $k = 3 \times 3$ in the form of an erode step followed by a dilation, allowing the removal of outliers. The cleaned regions are then filtered based on the size ratio compared to the total image size. Like this, objects containing less than 5% of the image’s pixels get discarded. Finally, a contour extraction is applied. During this last step, the average pixel value gets evaluated within every connected contour, the value of which is, in turn, used to determine the final region’s class. Based on this post-processing approach, the class noise is cleared out, as shown in Figure 5. Due to the overlapping char-

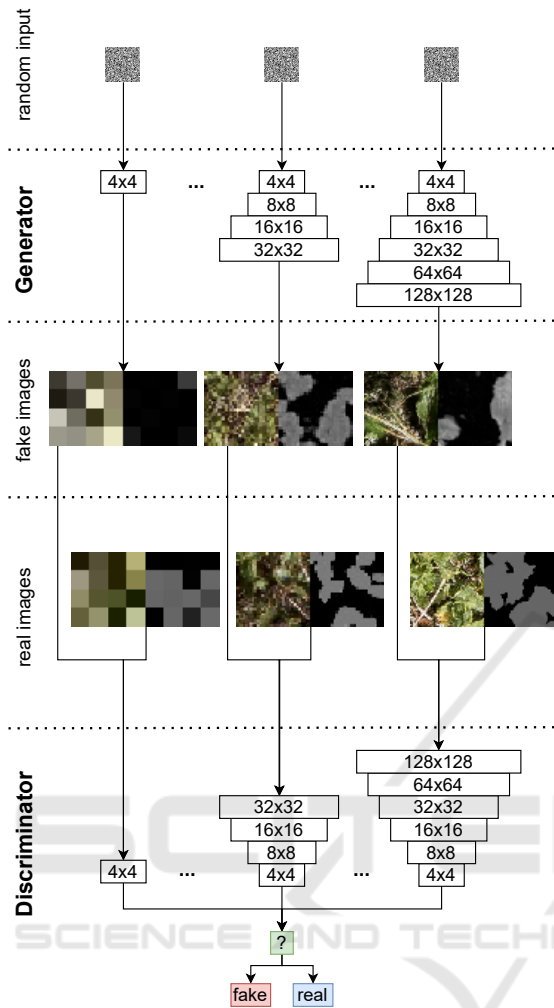


Figure 4: The Architecture of the Progressive Growing Generative Adversarial Network is shown with three example stages of the model with image sizes of 4×4 px, 32×32 px and 128×128 px. Based on random inputs, the respective generator stages create fake images, which are compared against authentic images from the training data set within the associated discriminator stage. Reconstructed from Figure 4 in (Zwettler et al., 2020).

acteristic of plants, the process partially results in a splitting of regions and, with this, in sometimes misclassified regions, which is also recognizable in the upper-central area of Figure 5c.

5 EVALUATION

The proposed process is evaluated based on the following three plant species in the created data set: *Soldanella pusilla*, *Gnaphalium supinum*, and *Euphrasia minima*. Due to the small reference data set, the evaluation uses a cross-validation approach, where

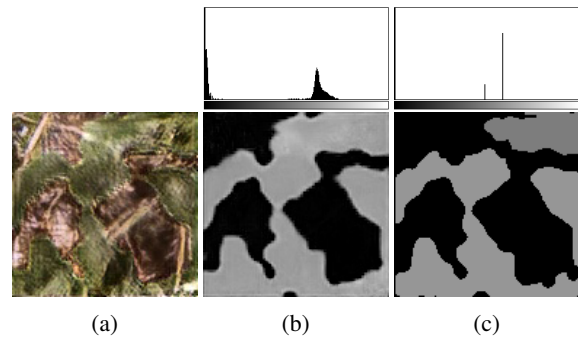


Figure 5: The GAN model's sample output shows (a) the resulting RGB image and (b) the associated classification mask with its histogram. Due to the noise in the created mask, region-based post-processing is applied, resulting in (c) an improved mask as highlighted by its histogram.

three randomly-selected images of the specific plant species get removed from the data set. The remaining images of the respective species are augmented and used to train a single-class U-Net model. Like this, only real-world images enter the model. Additionally, the data set of all species, excluding the three left-out images, is also augmented and used to train a PGGAN model. This model is, in turn, employed to generate 1000 artificial images containing the current plant species. The generated images are then augmented and used with the plant-specific images from the real-world data set to train another U-Net model. Based on the U-Net segmentation model trained from exclusively real-world images and the second model built up on real-world and artificial images, the evaluation involves the initially selected three images by comparing the segmentation accuracy. This process is done three times per plant species, with non-overlapping evaluation examples from the base data set, resulting in nine independent evaluation runs.

6 RESULTS

The confusion matrices associated with the evaluation results are listed in Table 2 per run and image, and summarized in Table 3 based on the Dice Score. Reading Table 3 shows an average Dice Score of 47.96% for the real-world model and an accuracy of 36.59% for the artificial model for *Soldanella pusilla*, 24.16% and 26.18% for *Gnaphalium supinum*, and 33.56% and 42.96% for *Euphrasia minima*.

The evaluation shows that the utilization of a generative approach, like a PGGAN model, can be used to enhance the data basis for the training of deep learning models for the segmentation of fuzzy structures such as in plant species. Although, this is not

Table 2: Relative confusion matrix of the evaluation, showing the individual results of the runs and the associated images based on the (in-)correctly detected foreground (FG) and background pixels (BG) in the resulting mask, compared to the ground truth (GT) mask. The matrix compares multiple runs using U-Net segmentation models that have been trained using real-world (RW) data only and such ones that have been trained using both real-world as well as artificial data (AD), which has been generated using a PGGAN model.

Run	Data		Image						
			1		2		3		
			FG	BG	FG	BG	FG	BG	
Soldanella pusilla	1	RW	FG (GT)	0.63	0.37	0.21	0.79	0.01	0.99
		BG (GT)	0.01	0.99	0.01	0.99	0.00	1.00	
	AD	FG (GT)	0.41	0.59	0.03	0.97	0.00	1.00	
		BG (GT)	0.00	1.00	0.00	1.00	0.00	1.00	
	2	RW	FG (GT)	0.51	0.49	0.52	0.48	0.00	1.00
		BG (GT)	0.01	0.99	0.00	1.00	0.00	1.00	
	AD	FG (GT)	0.31	0.69	0.27	0.73	0.04	0.96	
		BG (GT)	0.00	1.00	0.00	1.00	0.00	1.00	
	3	RW	FG (GT)	0.53	0.47	0.49	0.51	0.56	0.44
BG (GT)			0.00	1.00	0.01	0.99	0.01	0.99	
AD		FG (GT)	0.45	0.55	0.41	0.59	0.37	0.63	
		BG (GT)	0.00	1.00	0.00	1.00	0.00	1.00	
Gnaphalium supinum	1	RW	FG (GT)	0.17	0.83	0.28	0.72	0.00	1.00
		BG (GT)	0.00	1.00	0.00	1.00	0.00	1.00	
	AD	FG (GT)	0.33	0.67	0.10	0.90	0.00	1.00	
		BG (GT)	0.02	0.98	0.01	0.99	0.00	1.00	
	2	RW	FG (GT)	0.69	0.31	0.28	0.72	0.01	0.99
		BG (GT)	0.00	1.00	0.00	1.00	0.00	1.00	
	AD	FG (GT)	0.71	0.29	0.38	0.62	0.05	0.95	
		BG (GT)	0.00	1.00	0.00	1.00	0.01	0.99	
	3	RW	FG (GT)	0.04	0.96	0.02	0.98	0.08	0.92
BG (GT)			0.00	1.00	0.00	1.00	0.00	1.00	
AD		FG (GT)	0.00	1.00	0.19	0.81	0.05	0.95	
		BG (GT)	0.00	1.00	0.00	1.00	0.01	0.99	
Euphrasia minima	1	RW	FG (GT)	0.50	0.50	0.23	0.77	0.40	0.60
		BG (GT)	0.01	0.99	0.01	0.99	0.02	0.98	
	AD	FG (GT)	0.51	0.49	0.21	0.79	0.51	0.49	
		BG (GT)	0.00	1.00	0.01	0.99	0.01	0.99	
	2	RW	FG (GT)	0.79	0.21	0.35	0.65	0.52	0.48
		BG (GT)	0.01	0.99	0.00	1.00	0.01	0.99	
	AD	FG (GT)	0.89	0.11	0.53	0.47	0.26	0.74	
		BG (GT)	0.01	0.99	0.00	1.00	0.00	1.00	
	3	RW	FG (GT)	0.59	0.41	0.76	0.24	0.11	0.89
BG (GT)			0.01	0.99	0.03	0.97	0.00	1.00	
AD		FG (GT)	0.38	0.62	0.65	0.35	0.19	0.81	
		BG (GT)	0.00	1.00	0.02	0.98	0.00	1.00	

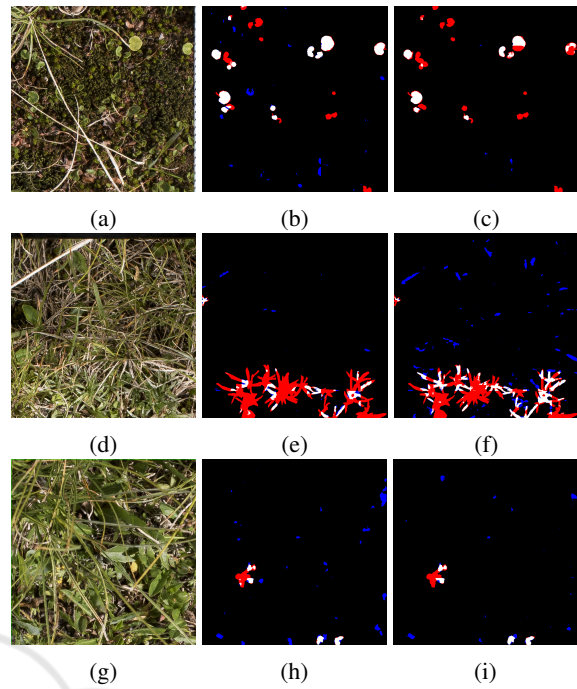


Figure 6: Evaluation results of the first image per first run from Table 2 for *Soldanella pusilla* with (a, b, c), *Gnaphalium supinum* with (d, e, f) and *Euphrasia minima* with (g, h, i). The first column shows the randomly selected images from the data set. The second column shows the raw segmentation results of the real-world-only U-Net model and the third column the raw results of the second model, which is also based on artificial images. The segmentation results are shown without the proposed post-processing step. Values that are classified as true-positives are shown in white, true-negatives in black, false-positives in blue and false-negatives in red.

applicable for all plant species, as shown with *Soldanella pusilla* in the evaluation, the results are improved for *Gnaphalium supinum* and especially for *Euphrasia minima*. These results are linked to the used data set. The images generated using the PGGAN model share similar features, that have been isolated during the models’ training, with the real world images. Regardless of that, the visual quality is not comparable to their real world counterparts, because of the small training data set. This is particularly evident for *Soldanella pusilla* as the most prominent of the ten available plant species with a comparable huge training data set of 162 images, where the additional, artificial and not-photorealistic images dilute the high quality real-world images. On the other hand, the amount of examples available for *Euphrasia minima* are massively smaller with only 23 available images, through which the utilization of additional, artificial data shows more advantages. While *Gnaphalium supinum* is with 103 occurrences in between of

Table 3: Evaluation results comparing the U-Net models based on real-world data only and the models, that are also trained using additional artificial images, which are created using a PGGAN model.

Run	Soldanella pusilla		Gnaphalium supinum		Euphrasia minima	
	Dice Score (Real-World)	Dice Score (Artificial)	Dice Score (Real-World)	Dice Score (Artificial)	Dice Score (Real-World)	Dice Score (Artificial)
1	35.92%	21.27%	23.17%	19.22%	32.86%	45.53%
2	44.38%	30.86%	41.75%	46.06%	28.65%	39.76%
3	63.57%	57.64%	7.56%	13.24%	39.19%	46.60%
Avg	47.96%	36.59%	24.16%	26.18%	33.56%	42.96%

the other two plant species, also the improvements of the second segmentation models get smaller. Figure 6 visually highlights the raw results for the first image of every first run listed in Table 2, where the additional, artificial training data leads to less false-positive results for *Euphrasia minima* (cf. Figure 6h and 6i) and an increased amount of true-positives, but also an increasing number of false-positives for *Gnaphalium supinum* (cf. Figure 6e and 6f). Additionally, the *Soldanella pusilla* example shows an increased number of false-negatives, while decreasing the amount of false-positives (cf. Figure 6b and 6c).

7 CONCLUSION

The utilization of artificial data shows promise for training deep learning models in the context of segmenting fuzzy structures such as alpine plants. Especially for application areas with only a few pre-segmented examples available for training, architectures such as PGGAN widen the data set and improve results, as shown in the context of segmentation. Due to the separation in multiple models, instead of using a combined architecture as proposed by Dong et al. (Dong et al., 2019), this approach meets the requirements of sustainable artificial intelligence (AI) defined by the European Union. Since a separate model is given for each plant species, the portfolio to be segmented and classified can be expanded at any time. Otherwise, the training for a cumulative deep learning model would have to be trained each time for each adaptation, using immense amounts of energy. The fragmentation into separate models supports another premise of the European Union regarding machine learning and AI, namely explainability. By dividing the task into separate models, good technological conditions are created to support explainable AI.

In the future, we plan to increase the number of tests further. The behaviour of the approach will be tested for taller plants such as *Scorzoneroides helvetica*. Additional plant species will be included as they become available.

ACKNOWLEDGMENTS

Our thanks to the province of Upper Austria for facilitating the project AlpinIO with the easy2innovate funding program.

REFERENCES

- Antoniou, A., Storkey, A., and Edwards, H. (2017). Data augmentation generative adversarial networks. *arXiv preprint arXiv:1711.04340*.
- Brunetti, M., Magoga, G., Iannella, M., Biondi, M., and Montagna, M. (2019). Phylogeography and species distribution modelling of *cryptocephalusbarii* (coleoptera: Chrysomelidae): is this alpine endemic species close to extinction? *ZooKeys*, 856:3.
- Chen, X., Li, Y., Yao, L., Adeli, E., and Zhang, Y. (2021). Generative adversarial u-net for domain-free medical image augmentation. *arXiv e-prints*, pages arXiv–2101.
- Creswell, A., White, T., Dumoulin, V., Arulkumaran, K., Sengupta, B., and Bharath, A. A. (2018). Generative adversarial networks: An overview. *IEEE Signal Processing Magazine*, 35(1):53–65.
- Dirnböck, T., Dullinger, S., and Grabherr, G. (2003). A regional impact assessment of climate and land-use change on alpine vegetation. *Journal of Biogeography*, 30(3):401–417.
- Dong, X., Lei, Y., Wang, T., Thomas, M., Tang, L., Curran, W. J., Liu, T., and Yang, X. (2019). Automatic multiorgan segmentation in thorax ct images using u-net-gan. *Medical physics*, 46(5):2157–2168.
- Eberl, T. and Kaiser, R. (2020). *Monitoring- und Forschungsprogramm zur langfristigen Ökosystembeobachtung im Nationalpark Hohe Tauern*. Verlag der Österreichischen Akademie der Wissenschaften.
- Engler, R., Randin, C. F., Thuiller, W., Dullinger, S., Zimmermann, N. E., Araújo, M. B., Pearman, P. B., Le Lay, G., Piedallu, C., Albert, C. H., et al. (2011). 21st century climate change threatens mountain flora unequally across europe. *Global Change Biology*, 17(7):2330–2341.
- Fadnavis, S. (2014). Image interpolation techniques in digital image processing: an overview. *International*

- Journal of Engineering Research and Applications*, 4(10):70–73.
- Gobbi, M., Ambrosini, R., Casarotto, C., Diolaiuti, G., Ficaretola, G., Lencioni, V., Seppi, R., Smiraglia, C., Tampucci, D., Valle, B., et al. (2021). Vanishing permanent glaciers: climate change is threatening a european union habitat (code 8340) and its poorly known biodiversity. *Biodiversity and Conservation*, 30(7):2267–2276.
- Guo, X., Chen, C., Lu, Y., Meng, K., Chen, H., Zhou, K., Wang, Z., and Xiao, R. (2020). Retinal vessel segmentation combined with generative adversarial networks and dense u-net. *IEEE Access*, 8:194551–194560.
- Karras, T., Aila, T., Laine, S., and Lehtinen, J. (2018). Progressive growing of gans for improved quality, stability, and variation. In *International Conference on Learning Representations*.
- Kingma, D. P. and Ba, J. (2014). Adam: A method for stochastic optimization. In *International Conference on Learning Representations*.
- Körner, C. (2012). *Alpine Treelines*. Springer.
- Körner, C., Berninger, U., Daim, A., Eberl, T., Fernández Mendoza, F., Füreder, L., Grube, M., Hainzer, E., Kaiser, R., Meyer, E., Newesely, C., Niedrist, G., Petermann, J., Seeber, J., Tappeiner, U., and Wickham, S. (in press 2022). Long-term monitoring of high elevation terrestrial and 2 aquatic ecosystems in the alps – a five-year synthesis. *ecomont*, 14:44–65.
- Körner, C. and Hiltbrunner, E. (2021). Why is the alpine flora comparatively robust against climatic warming? *Diversity*, 13:1–15.
- Ronneberger, O., Fischer, P., and Brox, T. (2015). U-net: Convolutional networks for biomedical image segmentation. In *International Conference on Medical image computing and computer-assisted intervention*, pages 234–241. Springer.
- Rother, C., Kolmogorov, V., and Blake, A. (2004). ” grab-cut” interactive foreground extraction using iterated graph cuts. *ACM transactions on graphics (TOG)*, 23(3):309–314.
- Rubel, F., Brugger, K., Haslinger, K., Auer, I., et al. (2017). The climate of the european alps: Shift of very high resolution köppen-geiger climate zones 1800–2100. *Meteorologische Zeitschrift*, 26(2):115–125.
- Rukundo, O. and Cao, H. (2012). Nearest neighbor value interpolation. *International Journal of Advanced Computer Science and Applications*, 3(4):25–30.
- Rumpf, S. B., Hülber, K., Wessely, J., Willner, W., Moser, D., Gattringer, A., Klöner, G., Zimmermann, N. E., and Dullinger, S. (2019). Extinction debts and colonization credits of non-forest plants in the european alps. *Nature communications*, 10(1):1–9.
- Sandfort, V., Yan, K., Pickhardt, P. J., and Summers, R. M. (2019). Data augmentation using generative adversarial networks (cyclegan) to improve generalizability in ct segmentation tasks. *Scientific reports*, 9(1):1–9.
- Schonfeld, E., Schiele, B., and Khoreva, A. (2020). A u-net based discriminator for generative adversarial networks. In *Proceedings of the IEEE/CVF Conference on Computer Vision and Pattern Recognition*, pages 8207–8216.
- Shukla, P., Skea, J., Calvo Buendia, E., Masson-Delmotte, V., Pörtner, H., Roberts, D., Zhai, P., Slade, R., Connors, S., Van Diemen, R., et al. (2019). Ipcc, 2019: Climate change and land: an ipcc special report on climate change, desertification, land degradation, sustainable land management, food security, and greenhouse gas fluxes in terrestrial ecosystems. *Intergovernmental Panel on Climate Change (IPCC)*.
- Sommer, C., Malz, P., Seehaus, T. C., Lippl, S., Zemp, M., and Braun, M. H. (2020). Rapid glacier retreat and downwasting throughout the european alps in the early 21 st century. *Nature communications*, 11(1):1–10.
- Steinbauer, K., Lamprecht, A., Winkler, M., Di Cecco, V., Fasching, V., Ghosn, D., Maringer, A., Remoundou, I., Suen, M., Stanisci, A., Venn, S., and Pauli, H. (2022). Recent changes in high-mountain plant community functional composition in contrasting climate regimes. *Science of The Total Environment*, 829:154541.
- Sun, C., Shrivastava, A., Singh, S., and Gupta, A. (2017). Revisiting unreasonable effectiveness of data in deep learning era. In *Proceedings of the IEEE international conference on computer vision*, pages 843–852.
- Zwettler, G. A., Holmes III, D. R., and Backfrieder, W. (2020). Strategies for training deep learning models in medical domains with small reference datasets. *Journal of WSCG*. 2020.